

Hall conductivity of a Sierpiński carpet

Askar A. Iliasov^{1,2,*}, Mikhail I. Katsnelson¹ and Shengjun Yuan^{2,1,†}

¹*Institute for Molecules and Materials, Radboud University, Heyendaalseweg 135, 6525AJ Nijmegen, The Netherlands*

²*Key Laboratory of Artificial Micro- and Nano-structures of Ministry of Education and School of Physics and Technology, Wuhan University, Wuhan 430072, China*



(Received 22 July 2019; revised manuscript received 10 December 2019; published 13 January 2020)

We calculate the Hall conductivity of a Sierpiński carpet using Kubo-Bastin formula. The quantization of Hall conductivity disappears when we increase the depth of the fractal, and the Hall conductivity is no more proportional to the Chern number. Nevertheless, these quantities behave in a similar way showing some reminiscence of a topological nature of the Hall conductivity. We also study numerically the bulk-edge correspondence and find that the edge states become less manifested when the depth of Sierpiński carpet is increased.

DOI: [10.1103/PhysRevB.101.045413](https://doi.org/10.1103/PhysRevB.101.045413)

I. INTRODUCTION

Fractals were very popular in 1980 and various properties of fractals were intensively studied at that time [1–3]. Most of these works were focused on classical fractal systems; at the same time, it turned out that quantum properties of fractals are also unusual and interesting. For example, some fractals have the Cantor-like energy spectrum, which makes them similar to quasicrystals [4]. These studies of quantum properties of fractal structures were of purely theoretical interest. With recent technological advances, fractals can be produced by both nanofabrication methods and manipulation of individual molecules on metal surfaces [5–8]. This enhances the interest in a deeper understanding of the field. Recent theoretical works concerning quantum effects in fractals consider transport properties [9–11], plasmons [12], Anderson localization [13,14], topological properties [15–18], and other related topics [19–23]. The transport properties of electrons roaming in a fractional space are of great interest due to their possible experimental applications and deep connection with topological properties, which definitely deserve more attention.

The relation between conductivity and topological properties was established in a seminal work [24] by Thouless *et al.* It was shown that the off-diagonal (Hall) conductivity of two-dimensional electron gas in a perpendicular magnetic field is proportional to the topological invariant called Chern number. The derivation in Ref. [24] relies on the translational invariance of the system, thus the theory cannot be directly applied to quasiperiodic or fractal structures. For quasiperiodic systems, one can obtain nontrivial topological properties of Hall conductivity by looking at the Brillouin zone as a noncommutative manifold [25–27]. The same is true for disordered systems [28,29]. To our knowledge, the relation between Hall conductivity and Chern number is still

an open question for the case of fractal. A clarification of this issue could also provide a better understanding of fractional topological order, another hot subject in condensed matter physics [30,31].

It is also known for the systems with integer dimensions that the quantization of Hall conductivity is closely related to the existence of edge states, in the form of the so-called bulk-edge correspondence [32–34]. The terms *edge* and *bulk* can be well defined for systems without holes, or, at least, for a system, which has an integer dimension and finite number of holes. On the other hand, an infinite fractal has an infinite number of holes, and the distribution of these holes is very dense. Therefore the difference between edge states and bulk states and their connections to the quantization of Hall conductivity should be carefully checked. As an infinite fractal is not numerically reachable, a practical way is to study various approximations of finite fractals with holes of different scales.

In a recent work [15] Chern numbers of a Sierpiński carpet were calculated numerically. The authors found that the Chern numbers are quantized in some energy regions; in this sense, fractals still can possess nontrivial topological properties. They also studied Hall conductivity by calculating the variance of level spacings using the random matrix theory. However, the applicability of this approach to fractal is questionable, since the latter, strictly speaking, is not a disordered system. It was shown that the level-spacing distribution for some kind of fractals and quasiperiodic systems can have power-law behavior which cannot be described within the conventional random matrix theory [35–37]. Even if one can apply the latter to the spectrum of Sierpiński carpet, it is not enough to make a definite conclusion on the quantization of Hall conductivity. Hence, the variance of level spacing distribution is not the most reliable quantity to study the localization and quantization of Hall conductivity in fractals, and one needs to calculate them directly, if possible.

In this work we examine relations between Hall conductivity and topological properties of Sierpiński carpets. In order to do this, we calculate numerically the Hall conductivity and the so-called quasideigenstates for various iterations of Sierpiński

*A.Iliasov@science.ru.nl

†s.yuan@whu.edu.cn

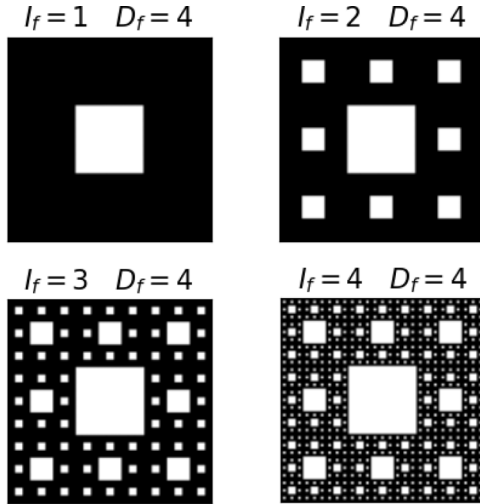


FIG. 1. The examples of studied fractal structures. The size of the large square is $3^{D_f} \times 3^{D_f}$ sites with $D_f = 4$ and different number of iterations I_f . With every iterations, new holes are deleted. The size of the smallest holes is $3^{D_f - I_f} \times 3^{D_f - I_f}$.

carpets and investigate their relations to the fractal depth. We also compare our results with the recently calculated Chern numbers obtained in Ref. [15].

II. THE MODEL

To study fractal structures, we use the single-orbital tight-binding Hamiltonian in the nearest-neighbor approximation, that is, the same model as in Refs. [9,10]:

$$H = -t \sum_{\langle ij \rangle} e^{i\phi_{ij}} c_i^\dagger c_j, \quad (1)$$

where c_i^\dagger creates fermion on a lattice site i , and $\langle ij \rangle$ denotes the nearest-neighbor sites belonging to the studied fractal. The influence of magnetic field is introduced by the standard Peierls substitution: $\phi_{ij} = 2\pi/\Phi_0 \int_{i,j}^j \mathbf{A} \cdot \mathbf{dr}$, where \mathbf{A} is the vector potential and $\Phi_0 = hc/e$ is the flux quantum. We use Landau gauge $\mathbf{A} = (-By, 0, 0)$.

We start with a square lattice of the size $3^{D_f} \times 3^{D_f}$. Then, we iteratively add holes, which gives us the realizations of Sierpiński carpet with varying depths. At first, we add the central hole of size $3^{D_f-1} \times 3^{D_f-1}$, then we add holes with size $3^{D_f-2} \times 3^{D_f-2}$, and so on. We can stop at any number of iterations I_f less than D_f and the maximum depth of fractal on a given lattice is D_f . If $I_f = D_f$, the size of a hole is equal to one site. Examples of different iterations are given in Fig. 1.

These structures have two parameters I_f and D_f , which describe various approximations of Sierpiński carpet. They also represent a transition from the usual square lattice with dimension 2 to a Sierpiński carpet with fractional dimension equal to $\ln 8 / \ln 3$.

In order to calculate the density of states and Hall conductivity we use the real-space approaches described in Refs. [38–41]. Using these methods, we are able to calculate electronic properties for six iterations of Sierpiński carpet without any diagonalization.

III. RESULTS

A. Density of states

We calculate density of states (DoS) for different fractal depths and iterations using a method based on the time evolution operator [38,39]. We start the evolution of a quantum system with a random initial state $|\psi\rangle$, which is normalized so that $|\psi|^2 = 1$. The density of states is calculated via Fourier transform of the correlation functions by averaging over initial random samplings [38,39]:

$$\begin{aligned} d(\epsilon) &= \langle \psi | \delta(\epsilon - H) | \psi \rangle \\ &= \frac{1}{2\pi} \int_{-\infty}^{+\infty} e^{i\epsilon\tau} \langle \psi | e^{-i\tau H} | \psi \rangle d\tau. \end{aligned}$$

Since density of states is a self-averaged quantity, it does not depend on the choice of the state $|\psi\rangle$ for large enough systems.

In Fig. 2, we show the calculated density of states for various magnetic fields with Φ/Φ_0 changing from 0 to 0.5, and here Φ is the magnetic flux through the smallest element for a given structure. The energy E is measured in values of hopping t of the Hamiltonian (1). These pictures of Hofstadter butterflies [42] are calculated for $D_f = 6$ and $I_f = 0, 2, 4, 5$ in Fig. 2, which demonstrates fractal structure of states and gaps due to additional period in hoppings associated with the magnetic flux.

From these pictures one can see that for $I_f = 0, 2, 4$ DoS is basically the same for all magnetic fields. The structure of Hofstadter butterfly with $I_f = 5$ is different from the previous cases. Many more states appear and small gaps open for some magnetic fields [new red lines and white dots in Fig. 2(d)]. Therefore, $I_f = 5$ seems to be the minimal depth that is needed to catch the peculiarities of quantum states in this particular fractal.

In Fig. 3, DoS is displayed for fractals with $I_f = 5, D_f = 6$ and $I_f = D_f = 6$, $\Phi/\Phi_0 = 0.25$. The change from $I_f = 5$ to $I_f = 6$ is clear: A gap opens in the middle of the spectrum, and there are more states between peaks (around energy $E = 2$). Density of states for $I_f = 5$ is flatter in that region.

We also calculated DoS for $I_f = D_f = 4$ and $I_f = D_f = 5$. The results are visually almost indistinguishable from $I_f = D_f = 6$. Hence, DoS converges for samples with maximum number of iterations and approaches the thermodynamic limit of a full fractal. For cases with $I_f < D_f < 6$ we also observe that DoS changes only a little while a transition to another regime occurs when changing from $I_f < D_f - 1$ to $I_f = D_f - 1$. Due to this transition, one cannot properly approximate the full fractal, if the smallest holes are absent in the sample.

The occurrence of the transition can be explained by the following reason. Before reaching the transition point the sample can still be treated as a bulk and the effective dimension is an integer. The holes in the sample can be seen as some additional disorders. When I_f is equal to 5 the distance between holes becomes comparable to the size of a site. Only at this point, the effective dimension of a sample becomes noninteger. The difference between cases $I_f = 5$ and $I_f = 6$ also can be explained by the difference in their noninteger

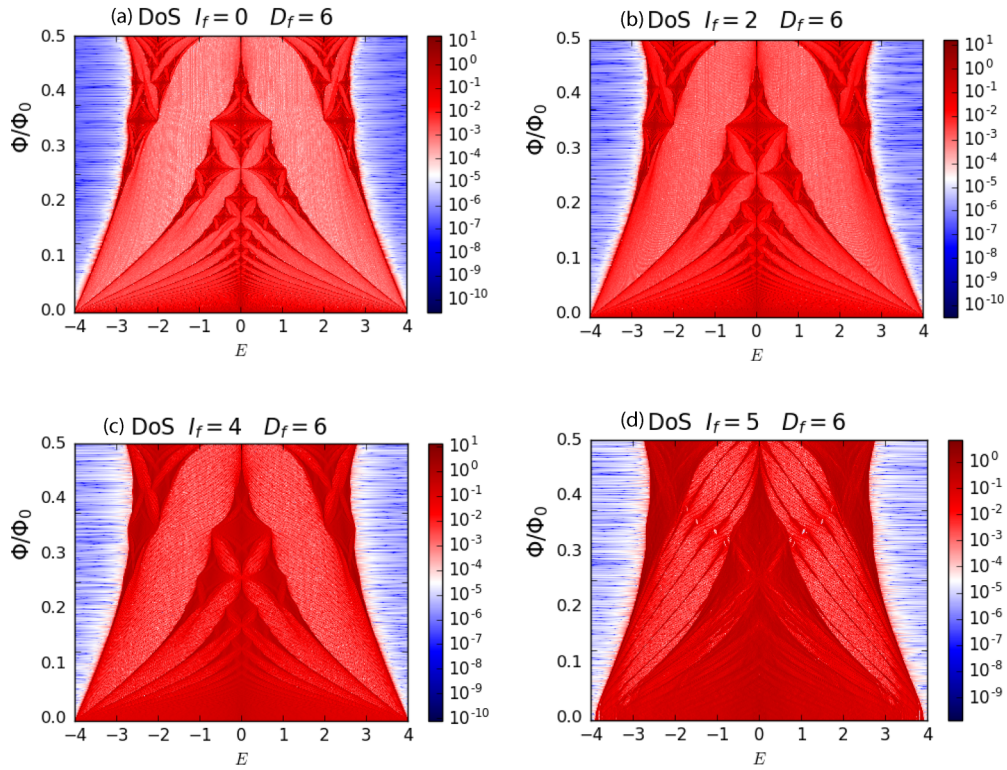


FIG. 2. Pictures of DoS depending on magnetic field—Hofstadter butterflies (magnetic field B corresponds to variations of Φ/Φ_0 from 0 to 0.5) for different iterations of Sierpiński carpet in a square of size $3^{D_f} \times 3^{D_f}$ and $D_f = 6$: (a) shows $I_f = 0$ iteration, (b) shows $I_f = 2$ iterations, (c) shows $I_f = 4$ iterations, (d) shows $I_f = 5$ iterations. The differences between (a), (b), and (c) are small. New peaks and gaps appear in the picture (d).

dimensions. Proper approximation to Sierpiński carpet is only achieved when $I_f = D_f$.

Let us consider a square with one hole $I_f = 1$ and then increase the number of sites D_f . This is an approximation of a two-dimensional system. The cases of $D_f = 1$ and $D_f = 2$ correspond to the Sierpiński carpets with $D_f = I_f$ and $D_f = I_f - 1$, since the average distances between holes are 1 site and 3 sites. These systems do not behave as two-dimensional systems: $D_f = I_f = 1$ is just a one-dimensional cycle. However, in the case of $I_f = 1$, for $D_f = 3$, the sample already has DoS similar to a two-dimensional sample. Therefore, we assume that samples with $I_f < D_f - 1$ approximate systems with integer dimensions and the transition of physical parameters should happen when $I_f = D_f - 1$.

We can think about this effect as a crucial property of exact scaling symmetry of fractals. Even the smallest breakage of scaling symmetry leads to an effective integer dimension rather than fractional. Every site is an edge site in a sample with maximum fractal depth. This condition strongly restricts the geometry of paths in the sample. We can assume therefore that the scaled geometry plays a decisive role in the properties of a fractal and it is closely connected to the space of paths in Sierpiński carpet.

B. Hall conductivity

In order to calculate Hall conductivity, we use the approach from Refs. [40,41]. The method is based on the so-called

Kubo-Bastin formula:

$$\sigma_{\alpha\beta} = \frac{i\hbar e^2}{A} \int_{-\infty}^{+\infty} d\epsilon f(\epsilon) \text{Tr} \left\langle v_\alpha \delta(\epsilon - H) v_\beta \frac{dG^+(\epsilon)}{d\epsilon} - v_\alpha \delta(\epsilon - H) v_\beta \frac{dG^-(\epsilon)}{d\epsilon} \right\rangle$$

where A is the area of the sample, $f(\epsilon) = \frac{1}{\exp(\epsilon - \mu)/T}$ is the Fermi-Dirac distribution, T is the temperature, μ is the chemical potential, v_α is α component of velocity operator, and $G^\pm = 1/(\epsilon - H \pm i\eta)$ are the Green's functions. In this formula we also average over random samplings as we did for the density of states. We can expand Green's functions and delta function in Chebyshev polynomials and then for the conductivity we obtain:

$$\sigma_{\alpha\beta} = \frac{4\hbar e^2}{\pi A} \frac{4}{\Delta E^2} \int_{-1}^1 d\tilde{\epsilon} \frac{f(\tilde{\epsilon})}{(1 - \tilde{\epsilon}^2)^2} \sum_{m,n} \Gamma_{nm}(\tilde{\epsilon}) \mu_{m,n}^{\alpha\beta}(H) \quad (2)$$

where $\tilde{\epsilon}$ is rescaled energy within $[-1, 1]$, ΔE is the energy range of spectrum, $\mu_{m,n}^{\alpha\beta}(H)$ and $\Gamma_{nm}(\tilde{\epsilon})$ are described by the following formulas:

$$\Gamma_{nm}(\tilde{\epsilon}) = T_m(\tilde{\epsilon})(\tilde{\epsilon} - in\sqrt{1 - \tilde{\epsilon}^2}e^{in \arccos(\tilde{\epsilon})}) + T_n(\tilde{\epsilon})(\tilde{\epsilon} + im\sqrt{1 - \tilde{\epsilon}^2}e^{-im \arccos(\tilde{\epsilon})})$$

and

$$\mu_{m,n}^{\alpha\beta}(H) = \frac{g_m g_n}{(1 + \delta_{n0})(1 + \delta_m)}.$$

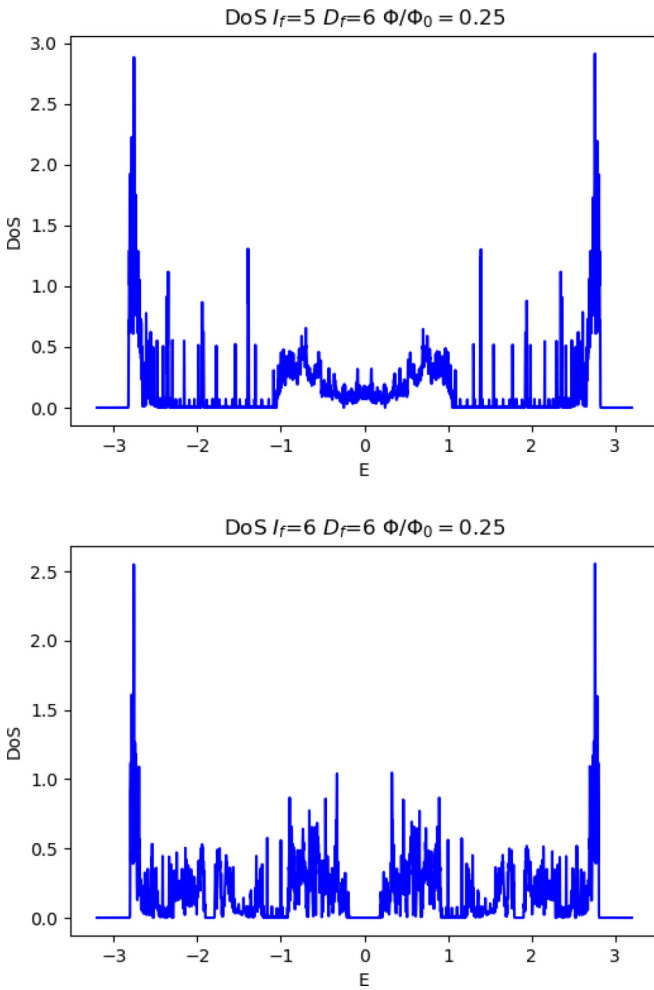


FIG. 3. The density of states for Sierpiński carpet with $I_f = 5$, $D_f = 6$ and $D_f = I_f = 6$ (maximum number of iterations for the square with size $3^6 \times 3^6$), $\Phi/\Phi_0 = 0.25$. A gap appears in the middle of the spectrum for $I_f = 6$, in comparison with $I_f = 5$.

We use Jackson kernel g_m to smooth Gibbs oscillations due to truncation of the expansion in Eq. (2) [40].

Our results for σ_{xy} are shown in Fig. 4. The Hall conductivity was calculated for $\Phi/\Phi_0 = 0.25$, $D_f = 6$, and $I_f = 0, 4, 5, 6$.

The Kubo-Bastin formula is derived under very general assumptions and can be used to study linear response for any Hamiltonian within single particle approximation. The only restriction of the formula is that it neglects the electron-electron interactions. For example, the Kubo-Bastin formula was successfully applied to systems with irregularities, such as disordered systems [40], which also lack translational symmetry, and it can be used for fractals as well.

The Hall conductivity behaves similarly to DoS, when changing the structure of the fractal. The differences between $I_f = 0$ and $I_f = 4$ are quite small, although there are more fluctuations in the case of $I_f = 4$. The profiles of the Hall conductivity are overall similar, for example, there are plateaus, which correspond to relatively small values of DoS, in the middle of the spectrum. These plateaus in Hall conductivity are related to topological invariants: Hall conductivity takes

value of e^2/h multiplied by the integer of the Chern number. One can see a clear transition at $I_f = 5$ iterations: The plateaus in the middle of the spectrum vanish at $I_f = 5$ and the fluctuations become much stronger.

The picture of Hall conductivity for $I_f = D_f = 6$ demonstrates a completely different behavior. We can compare these results to Chern numbers calculated in Ref. [15] [Fig. 3(c) in that article] for $I_f = D_f = 4$. In general, Hall conductivity looks similar to Chern numbers, however, there are more fluctuations and peaks that are absent in Chern numbers. One can also notice that plateaus appear on the scale $1.5e^2/h$, not e^2/h , which would be expected from values of Chern numbers on these energies. The exact plateaus of Chern numbers are located on the energies $E = -1.5 \dots -0.9$ and $E = 0.9 \dots 1.5$, and the almost quantized region is located around ± 2.5 with the width of the order of 0.1. These regions are highlighted in Fig. 4(d).

There are two regions which correspond to quantized Chern number, around $E = \pm 1$. These regions occur after smearing of peaks in smaller iteration depths I_f and for larger I_f they form regions resembling plateaus. The plateaus for smaller I_f are destroyed with increasing of I_f . There remain only small parts of them around $E = \pm 2.5$ and $E = \pm 1$, these regions correspond to almost quantized Chern number. It is interesting in the region around $E = \pm 1$ there is no plateau even with quantized Chern numbers. This has been checked with averaging from different numbers of random samples until fluctuations are stable. The central gap in DoS corresponds to conductivity $\sigma_{xy} = 0$, as well as the Chern number is equal to 0. Therefore, we can conclude that the relation between Chern numbers and Hall conductivity does not hold in noninteger dimensions, although there are similarities in their behavior. There is no quantized Hall conductivity plateaus as for Chern numbers, but, nevertheless, disturbed plateaus appear exactly in the regions of quantized Chern numbers.

We also checked the influence of disorders to the Landau level spectrum and Hall conductivity by introducing random vacancies in the samples. The results are shown in Fig. 5, where we deleted around 20% of the sites randomly. We see that the Hall conductivities are stable with respect to the disorder. Moreover, there are less fluctuations on the Hall conductivities in comparison with the results shown in Fig. 4. These results indicate that the Hall conductivities of fractals are stable under the presence of disorder as long as the strength of disorder is not very strong. This property is indeed the same as for systems with integer dimensions.

In fact, these results can be understood in a simple way. The holes in a pristine fractal can be regarded as a kind of disorder. Thus additional holes (single point vacancies) should not affect the physical properties unless the disorder is too large. However, there are still subtleties since the exact scaling symmetry on all scales is important for building a correct approximation of the fractal.

C. Quasieigenstates

It is known that the edge states in quantum Hall systems are closely related to their topological properties [32,33,43]. Occurrence of the edge states corresponds to quantized Chern numbers (bulk-edge correspondence). Therefore it is natural

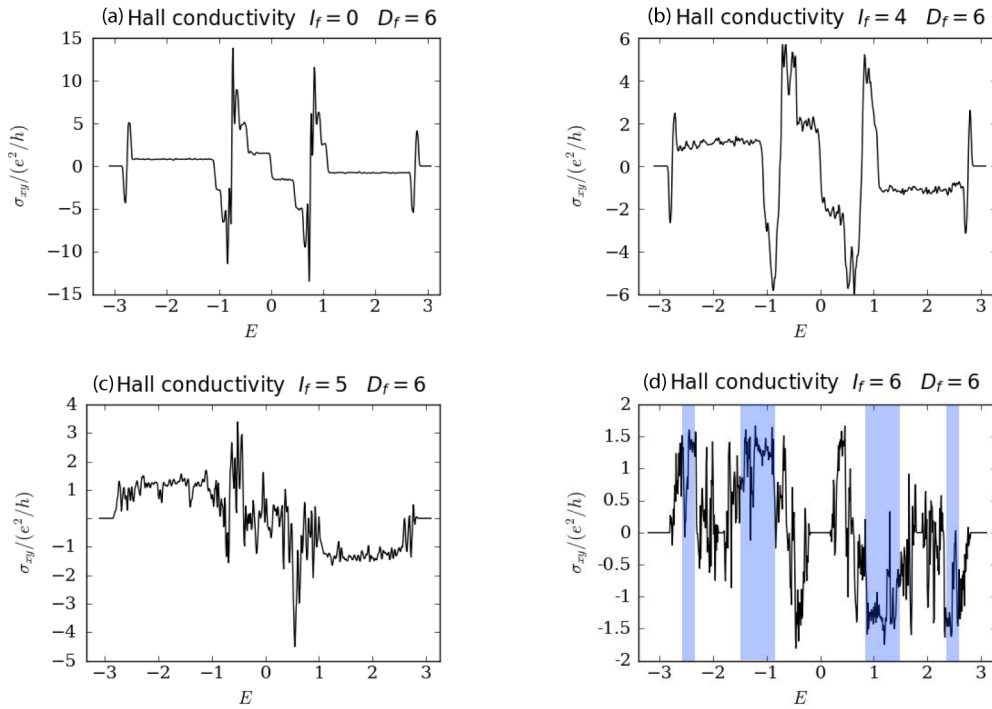


FIG. 4. The Hall conductivity for different iterations of Sierpiński carpet in a square of the size $3^{D_f} \times 3^{D_f}$ and $D_f = 6$ ($\Phi/\Phi_0 = 0.25$): (a) is $I_f = 0$ iteration, (b) is $I_f = 4$ iterations, (c) is $I_f = 5$ iterations, (d) is $I_f = 6$ iterations. As in Fig. 2, the differences between (a) and (b) are small; only small fluctuations are added in (b). Picture (c) demonstrates transition to another phase, picture (d) is very different from previous cases, the regions of quantized Chern numbers are shown by blue.

to assume that transitions with increasing I_f in DoS and Hall conductivity will be seen in the edge states as well. To explore this question we calculated quasieigenstates for Sierpiński carpet. Quasieigenstates and probability current were calculated by the same method of averaging [39]. For the probability current, we use the formula [44]:

$$\mathbf{j} = \text{Re}(\psi^* \mathbf{v} \psi) = \frac{\hbar}{m_e} \text{Im}(\psi^* \nabla \psi) - \frac{q}{m_e} \mathbf{A} |\psi|^2. \quad (3)$$

First, let us take a look at states corresponding to plateaus and peaks for some iterations with enough holes, but with regular behavior of Hall conductivity. For more readable pictures we used samples with size $D_f = 5$. Examples of bulk and edge states for $I_f = 3$ iterations are shown in Fig. 6. Edge states, which are shown on the left side of picture, correspond to energies $E = 1.51$ and $E = 2.59$. Bulk states, which are

shown on the right panels, correspond to energies $E = 1.09$ and $E = 2.83$. Edge states are taken from the regions with disturbed plateaus in Hall conductivity and bulk states from slopes of peaks. We see that edge states can be localized along holes on different scales i.e. only the central hole, holes of the second iteration and the central hole, all holes up to the third iteration and so on.

Examples of bulk and edge states for $I_f = 5$ iterations (i.e., fractal with maximum depth) are shown in Fig. 7. Edge states, which are shown on the left panels, correspond to energies $E = 1.33$ and $E = 2.59$. Bulk states, which are shown on the right panels, correspond to energies $E = 1.57$ and $E = 2.83$. The edge states on the left panel correspond to the region of quantized and almost quantized Chern number. There is a reminiscence of the quantization in Hall conductivity.

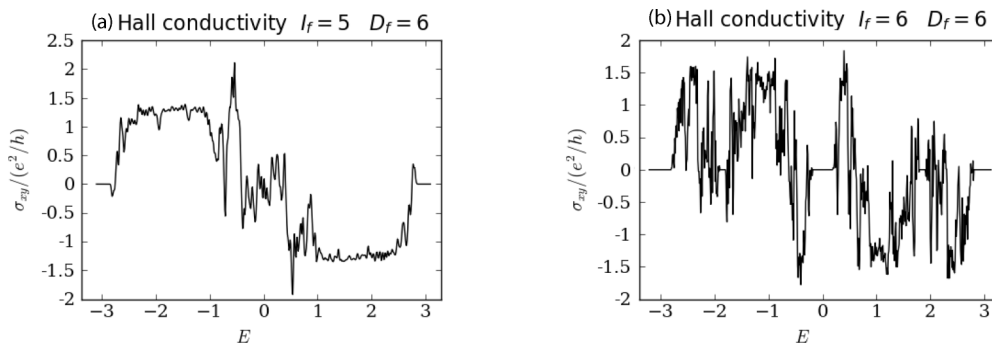


FIG. 5. The Hall conductivity for Sierpiński carpet with additional disorder in a square of the size $3^{D_f} \times 3^{D_f}$ and $D_f = 6$ ($\Phi/\Phi_0 = 0.25$): (a) is $I_f = 5$ iteration, (b) is $I_f = 6$ iterations. Approximately 20% of the sites are deleted. There are no visible differences from Fig. 4.

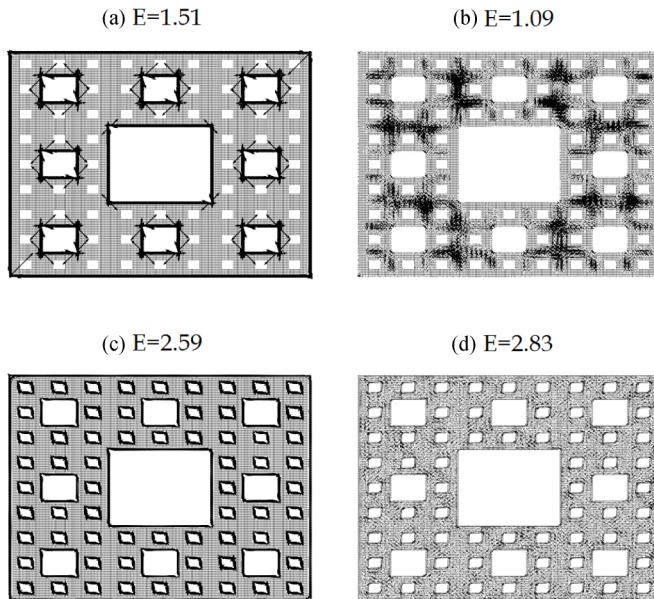


FIG. 6. Quasieigenstates for Sierpiński carpet with size $3^{D_f} \times 3^{D_f}$ with $D_f = 5$ and $I_f = 3$ iterations. Examples of edge states are on the left: picture (a) $E = 1.51$, picture (c) $E = 2.59$. Examples of bulk states are on the right: picture (b) $E = 1.09$, picture (d) $E = 2.83$.

We see that the edge states in the full fractal differ from the edge states in Fig. 6. In the sample with $I_f = 3$ iterations, the current is localized along borders in a homogeneous pattern, there are just lines of currents along the edges. However, in the full fractal, the current has a more complex pattern, for example, it can be localized around small holes, which are close to an edge. This deformation of edge current can be a

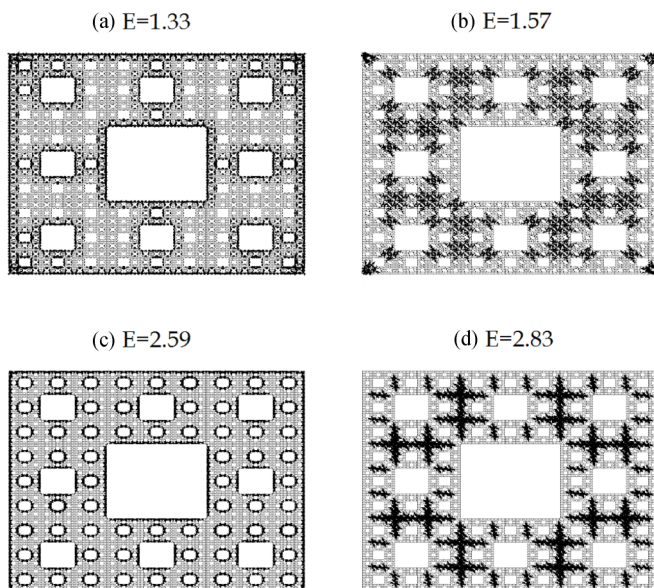


FIG. 7. Quasieigenstates for Sierpiński carpet with size $3^{D_f} \times 3^{D_f}$ with $D_f = 5$ and $I_f = 5$ iterations. Examples of edge states are on the left: picture (a) $E = 1.33$, picture (c) $E = 2.59$. Examples of bulk states are on the right: picture (b) $E = 1.57$, picture (d) $E = 2.83$.

reason of absence of flat plateaus in Hall conductivity even for regions with quantized Chern number. We also see that bulk states in a sample with $I_f = 5$ iterations demonstrate more symmetric behavior. This is, obviously, the manifestation of full scaling symmetry of a fractal.

We see that for the energies $E = 1.33$ and $E = 2.59$, which are in the regions of near-quantized and quantized Chern numbers, the edge states remain to be well defined. However, some part of plateaus of the previous iterations with the edge states become bulk states. We also see that some bulk states in different iterations have similar localization properties. Accordingly, we can assume that there are states with different effective scales. Some states spread over the rougher structure of a sample; some states sit only around smaller holes.

We have made calculations of quasi-for various energies and they all follow the described pattern. We see that the quasieigenstates corresponding to the quantized Hall conductivity are localized along the edges for iterations smaller than $I_f = 4$ (with maximum possible number of iterations equal to $D_f = 5$). It is also worth noticing that all edges, namely, the edges of the sample and the edges of the holes can contribute to quasieigenstates. For most quasieigenstates which have been calculated for various energies in the case of $I_f = 5$ and $D_f = 5$, there is no obvious domination of edge states.

Here, we observe the same transition of quasieigenstates as in DoS and Hall conductivity at $I_f = D_f - 1$ i.e. when the number of iterations is one less than the possible number of iterations. In the case of bulk states, it manifests as a more symmetric picture of the current. In the case of edge states, it manifests as a more complex localization along the edges, so that some edge states become localized along smaller holes, which are close to an edge.

IV. SUMMARY

We see that with increasing the depth of a fractal the quantization of Hall conductivity disappears. However, there is reminiscence of topological nature of quantization, namely some plateaus remain but disturbed. We also see that for Sierpiński carpet the general relation between topological invariants such as Chern numbers and Hall conductivity does not fulfill, contrary to the case of integer dimensions. The calculated conductivity is not proportional to the Chern number, but follows a similar pattern. Precisely, Hall conductivity is not an integer in units of e^2/h but exhibits disturbed plateaus in the regions where the Chern numbers are quantized. We speculate about possible reasons in the following.

At first, the formula, which calculates Chern number through projectors, was proven to be properly defined only for systems with translational invariance [45]. In the second, even if the formula works for fractals, it may only fulfill in the thermodynamic limit. Another reason behind the divergence of fractional and integer dimensions could be the definition of edge and bulk states. Some of the edge states are localized along inner holes in fractals. These states become closer to bulk states at maximal depth, therefore we cannot clearly distinguish, whether it is the localization along the edges or in the bulk due to inhomogeneities. Edge states along large holes also become localized not only along edges but also along small holes around an edge. These possible effects

on the quantization of Hall conductivity and its' relation to topological invariants require future investigation.

We also considered different iterations I_f of Sierpiński carpet on a fixed square sample with size $3^{D_f} \times 3^{D_f}$. We observed that there is a transition between two different regimes, which occurs when $I_f = D_f - 1$. This transition can be seen in density of states, Hall conductivity, and quasieigenstates. In the case of quasieigenstates, the edge states mostly become bulk states when I_f is increased. This result can be explained by the effective dimension. If the number of holes is finite, then the effective dimension of a sample is integer rather than fractional. The transition occurs when holes in a sample are dense enough and the effective dimension of the sample becomes noninteger.

Fractals have noninteger dimension with a dense set of holes and the proper definitions of edge and bulk states are not obvious. In order to clarify their connection to the quantization of Hall conductivity, we calculated quasieigenstates for different fractal depth. We observed that edge states can be localized along the borders of all holes of various scales, not only the edges of the sample. There is also no big difference in amplitudes of currents for different holes. Edge states still exist in a full fractal, but the behavior of their localization becomes different. Additional holes along the edges increase

effective localization width. Therefore, one can assume that if a state is localized around small holes and these holes are dense enough, there could be a transition from edge state to a bulk state. It could explain the result that despite the similarity between Hall conductivity and Chern numbers, plateaus in Hall conductivity are disturbed in fractals.

Note added. Recently, a preprint [46] appeared which treated a similar problem but in a technically different way (it was based on Landauer formula rather than Kubo-Bastin formula and did not include an analysis of edge states). Qualitatively, parts of our conclusions are similar to the conclusions obtained in that paper.

ACKNOWLEDGMENTS

We are thankful to Tom Westerhout for helpful discussions. This work was supported by the National Science Foundation of China under Grant No. 11774269 and by the Dutch Science Foundation NWO/FOM under Grant No.16PR1024 (S.Y.), and by the JTC-FLAGERA Project GRANSPOORT (M.I.K.). Support by the Netherlands National Computing Facilities foundation (NCF), with funding from the Netherlands Organisation for Scientific Research (NWO), is gratefully acknowledged.

-
- [1] S. Havlin and D. Ben-Avraham, Diffusion in disordered media, *Adv. Phys.* **36**, 695 (1987).
 - [2] L. Pietronero and E. Tosatti (Eds.), *Fractals in Physics* (Elsevier, Amsterdam, 1986).
 - [3] J. Feder, *Fractals* (Plenum Press, New York, 1988).
 - [4] E. Domany, S. Alexander, D. Bensimon, and L. Kadanoff, Solutions to the Schrödinger equation on some fractal lattices, *Phys. Rev. B* **28**, 3110 (1983).
 - [5] M. Polini, F. Guinea, M. Lewenstein, H. C. Manoharan, and V. Pellegrini, Artificial honeycomb lattices for electrons, atoms and photons, *Nat. Nanotechnol.* **8**, 625 (2013).
 - [6] M. Gibertini, A. Singha, V. Pellegrini, M. Polini, G. Vignale, A. Pinczuk, L. N. Pfeiffer, and K. W. West, Engineering artificial graphene in a two-dimensional electron gas, *Phys. Rev. B* **79**, 241406(R) (2009).
 - [7] J. Shang, Y. Wang, M. Chen, J. Dai, X. Zhou, J. Kuttner, G. Hilt, X. Shao, J. M. Gottfried, and K. Wu, Assembling molecular Sierpinski triangle fractals, *Nat. Chem.* **7**, 389 (2015).
 - [8] S. N. Kempkes, M. R. Slot, S. E. Freney, S. J. M. Zevenhuizen, D. Vanmaekelbergh, I. Swart, and C. Morais Smith, Design and characterization of electrons in a fractal geometry, *Nat. Phys.* **15**, 127 (2018).
 - [9] E. van Veen, S. Yuan, M. I. Katsnelson, M. Polini, and A. Tomadin, Quantum transport in Sierpinski carpets, *Phys. Rev. B* **93**, 115428 (2016).
 - [10] E. van Veen, A. Tomadin, M. Polini, M. I. Katsnelson, and S. Yuan, Optical conductivity of a quantum electron gas in a Sierpinski carpet, *Phys. Rev. B* **96**, 235438 (2017).
 - [11] Z.-G. Song, Y.-Y. Zhang, and S.-S. Li, The topological insulator in a fractal space, *Appl. Phys. Lett.* **104**, 233106 (2014).
 - [12] T. Westerhout, E. van Veen, M. I. Katsnelson, and S. Yuan, Plasmon confinement in fractal quantum systems, *Phys. Rev. B* **97**, 205434 (2018).
 - [13] D. Sticlet and A. Akhmerov, Attractive critical point from weak antilocalization on fractals, *Phys. Rev. B* **94**, 161115(R) (2016).
 - [14] A. Kosior and K. Sacha, Localization in random fractal lattices, *Phys. Rev. B* **95**, 104206 (2017).
 - [15] M. Brzezinska, A. M. Cook, and T. Neupert, Topology in the Sierpinski-Hofstadter problem, *Phys. Rev. B* **98**, 205116 (2018).
 - [16] A. Agarwala, S. Pai, and V. B. Shenoy, Fractalized metals, [arXiv:1803.01404](https://arxiv.org/abs/1803.01404).
 - [17] B. Pal, W. Wang, S. Manna, and A. E. B. Nielsen, Anyons and fractional quantum hall effect in fractal dimensions, [arXiv:1907.03193](https://arxiv.org/abs/1907.03193).
 - [18] S. Pai and A. Prem, Topological states on fractal lattices, *Phys. Rev. B* **100**, 155135 (2019).
 - [19] A. K. Golmankhaneh, Statistical mechanics involving fractal temperature, *Fractal Fract.* **3**, 20 (2019).
 - [20] I. Akal, Entanglement entropy on finitely ramified graphs, *Phys. Rev. D* **98**, 106003 (2018).
 - [21] B. Pal and K. Saha, Flat bands in fractal-like geometry, *Phys. Rev. B* **97**, 195101 (2018).
 - [22] A. Nandy and A. Chakrabarti, Engineering slow light and mode crossover in a fractal-kagome waveguide network, *Phys. Rev. A* **93**, 013807 (2016).
 - [23] A. Nandy, B. Pal, and A. Chakrabarti, Flat band analogues and flux driven extended electronic states in a class of geometrically frustrated fractal networks, *J. Phys.: Condens. Matter* **27**, 125501 (2015).
 - [24] D. J. Thouless, M. Kohmoto, M. P. Nightingale, and M. den Nijs, Quantized Hall Conductance in a Two-Dimensional Periodic Potential, *Phys. Rev. Lett.* **49**, 405 (1982).
 - [25] D.-C. Tran, A. Dauphin, N. Goldman, and P. Gaspard, Topological Hofstadter insulators in a two-dimensional quasicrystal, *Phys. Rev. B* **91**, 085125 (2015).

- [26] Y. E. Kraus and O. Zeitler, Topological Equivalence between the Fibonacci Quasicrystal and the Harper Model, *Phys. Rev. Lett.* **109**, 116404 (2012).
- [27] J. Bellissard, Gap labelling theorems for Schrödinger operators, in *From Number Theory to Physics*, edited by M. Waldschmidt, P. Moussa, J.-M. Luck, and C. Itzykson (Springer, Berlin, Heidelberg, 1992).
- [28] E. Prodan, Disordered topological insulators: a non-commutative geometry perspective, *J. Phys. A: Math. Theor.* **44**, 239601 (2011).
- [29] J. Bellissard, A. van Elst, and H. Schulz-Baldes The noncommutative geometry of the quantum Hall effect, *J. Math. Phys.* **35**, 5373 (1994).
- [30] G. B. Halász, T. H. Hsieh, and L. Balents, Fracton Topological Phases from Strongly Coupled Spin Chains, *Phys. Rev. Lett.* **119**, 257202 (2017).
- [31] T. Devakul, Y. You, F. J. Burnell, and S. L. Sondhi, Fractal symmetric phases of matter, *SciPost Phys.* **6**, 007 (2019).
- [32] B. I. Halperin, Quantized Hall conductance, current-carrying edge states, and the existence of extended states in a two-dimensional disordered potential, *Phys. Rev. B* **25**, 2185 (1982).
- [33] Y. Hatsugai, Chern Number and Edge States in the Integer Quantum Hall Effect, *Phys. Rev. Lett.* **71**, 3697 (1993).
- [34] R. S. K. Mong and V. Shivamoggi, Edge states and the bulk-boundary correspondence in Dirac Hamiltonians, *Phys. Rev. B* **83**, 125109 (2011).
- [35] A. A. Iliasov, M. I. Katsnelson, and S. Yuan, Power-law energy level spacing distributions in fractals, *Phys. Rev. B* **99**, 075402 (2019).
- [36] A. Hernando, M. Sulc, and J. Vanicek, Spectral properties of electrons in fractal nanowires, [arXiv:1503.07741v1](https://arxiv.org/abs/1503.07741v1).
- [37] K. Machida and M. Fujita, Quantum energy spectra and one-dimensional quasiperiodic systems, *Phys. Rev. B* **34**, 7367 (1986).
- [38] A. Hams and H. De Raedt, Fast algorithm for finding the eigenvalue distribution of very large matrices, *Phys. Rev. E* **62**, 4365 (2000).
- [39] S. Yuan, H. De Raedt, and M. I. Katsnelson, Modeling electronic structure and transport properties of graphene with resonant scattering centers, *Phys. Rev. B* **82**, 115448 (2010).
- [40] J. H. Garcia, L. Covaci, and T. G. Rappoport, Real-Space Calculation of the Conductivity Tensor for Disordered Topological Matter, *Phys. Rev. Lett.* **114**, 116602 (2015).
- [41] S. Yuan, E. van Veen, M. Katsnelson, and R. Roldan, Quantum Hall effect and semiconductor-to-semimetal transition in biased black phosphorus, *Phys. Rev. B* **93**, 245433 (2016).
- [42] D. R. Hofstadter, Energy levels and wave functions of Bloch electrons in rational and irrational magnetic fields, *Phys. Rev. B* **14**, 2239 (1976).
- [43] R. E. Prange and S. M. Girvin (Eds.), *The Quantum Hall effect* (Springer, Berlin, 1987).
- [44] K. Hornberger and U. Smilansky, Magnetic edge states, *Phys. Rep.* **367**, 249 (2002).
- [45] A. Kitaev, Anyons in an exactly solved model and beyond, *Ann. Phys.* **321**, 2 (2006).
- [46] M. Fremling, M. van Hooft, C. Morais Smith, and L. Fritz, Existence of robust edge currents in Sierpiński fractals, *Phys. Rev. Research* **2**, 013044 (2020).